Marine Geology, 69 (1985) 155—170
Elsevier Scientific Publishers B.V., Amsterdam — Printed in The Netherlands

THE QUANTITATIVE DESCRIPTION OF BEACH CYCLES*

DAVID G. AUBREY AND ROBERT M. ROSS**
Woods Hole Oceanographic Institution, Woods Hole, MA 02543 (U.S.A.)
(Received November 19, 1984; revised and accepted April 23, 1985)

ABSTRACT

Aubrey, D.G. and Ross, R.M., 1985. The quantitative description of beach cycles. Mar. Geol., 69: 155—170.

A quantitative method is developed to describe sequential changes in beach profile morphology. Dominant cycles in temporal eigenfunctions (computed by empirical eigenfunction analysis and rotary component analysis) are defined and used to construct a sequence of profiles representing the energetic portions of beach cycles. Five sets of beach profile data from Torrey Pines Beach in southern California were analyzed with these techniques. Because the first and second eigenfunctions account for between 65 and 90% of the variability of the data, the beach profiles are accurately described with only these two variables and the mean profile. Using rotary component analysis, beach changes represented by the two dominant eigenfunctions can be separated into many elliptical components, each representing a particular frequency associated with cycles in beach state. Profiles are reconstructed using points from the perimeter (latera recta) of these beach state ellipses.

A frequency of 1 cpy is the most energetic frequency in the first and second eigenfunctions, corresponding to the cyclic onshore—offshore sediment movement associated with "bar" and "berm" profiles. Profiles constructed from points on the elliptical path associated with annual cycles graphically depict the sequential development of bar and berm during the beach cycle. Beach cycles corresponding to a frequency of 2 cpy are also significant, primarily due to the energy of the second eigenfunction. No other frequencies are consistently found to be as significant as the annual and semi-annual cycles at this beach. In particular, monthly beach cycles have little energy associated with them.

The method described provides a uniform way to objectively discriminate energetic beach cycles, and yields a concise representation for beach modeling and prediction. It should be a valuable tool for uniform, quantitative intercomparison of beaches and beach cycles.

INTRODUCTION

Detailed knowledge of beach cycles is necessary for proper management of coastal resources, particularly in light of widespread coastal retreat. Previous models of sequential beach change have been mostly qualitative. Shepard (1950) performed some of the first detailed analyses of beach

*W.H.O.I. Contribution No. 5859.
**Present address: Harvard University, Cambridge, MA 02138, U.S.A.

0025-3227/85/$03.30

cycles, using observations from southern California. Sonu and Van Beek (1971) were among the first to postulate that morphological changes in beach profiles are a function of the pre-existing morphology, implying an ordered sequence of change. They developed a model, derived from analysis of one-half year of semidiurnal beach profile data measured on the Outer Banks, North Carolina, that predicted beach profile shape based on pre-existing sediment storage, beach width, and surface configuration.

Wright et al. (1979) proposed a qualitative model of systematic beach changes related to surf-zone dynamics, based on studies of Australian beaches. Short (1979) presented a three-dimensional descriptive model of beach- and surf-zone morphodynamic states, based also on field data from the Australian coast. Each state is associated with a level of breaker-wave power.

Wayland (1983) examined profile changes due to seasonality, storm cycles, and tides for one year of beach profile data from Duck, North Carolina. He plotted the first versus the second, and the third versus the fourth temporal eigenfunctions (computed with empirical eigenfunction analysis) and joined each successive profile survey. Wayland was able to identify the intervals of maximum profile change and match these to storm events that had occurred during the interval between profile data collection. In order to better understand the sediment movement associated with discrete points on the Cartesian plots, he reconstructed profiles representing points from each of the 4 quadrants for both eigenfunction 1 versus eigenfunction 2, and eigenfunction 3 versus eigenfunction 4. He concurred with Sonu and Van Beek (1971) that pre-existing morphology is an important factor in controlling subsequent profile changes.

Although this type of study has shown that the length and direction of vectors in "eigenspace" clarify the systematic changes of beach profiles, no one has attempted to construct a mean seasonal path through profile eigenspace. One could pick representative points from this mean path and quantitatively construct a sequence of beach profiles analogous to those determined by previous investigators. Such a sequence was the focus of this study, designed to quantitatively identify dominant cycles in beach development. Results described in this study are presented in more detail in Ross (1983).

Profiles were measured at Torrey Pines Beach, California, about 3 km north of Scripps Institution of Oceanography (Fig.1). The site is a 3 km long relatively straight sandy beach with simple nearshore bathymetry. Monthly data is available in two 5-year sets of profiles (from Indian Canyon Range and South Range) which extend from the backshore out to about 10 m below mean sea level, acquired from June 1972 to November 1977. Weekly data is available from Indian Canyon, North, and South Ranges from December 1975 to January 1977 (Aubrey, 1978), and includes a mixture of onshore/offshore and solely onshore profiles. Survey techniques are described in Aubrey (1979).

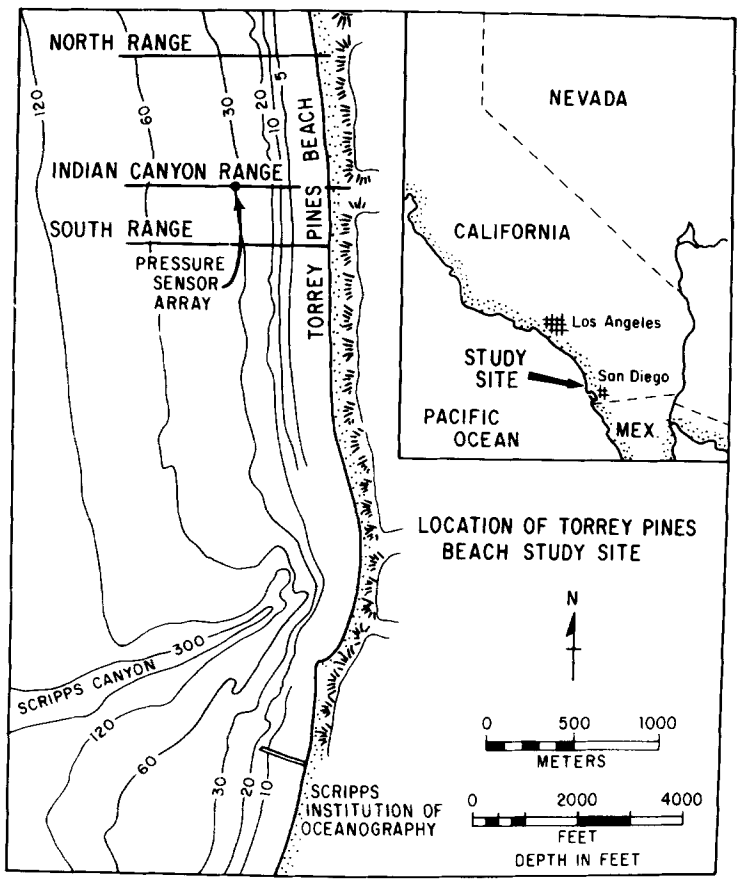

Fig.1. Map showing location of Torrey Pines Beach and the major rangelines (after Nordstrom and Inman, 1975).

METHODS

Empirical eigenfunction analysis (principal component analysis) was used to transform beach profile data, which is a set of intercorrelated variables, into a set of statistically independent variables. The new variables are linear combinations of the original variables, but are mutually orthogonal (uncorrelated). Eigenanalysis separates the temporal and spatial dependence of the data, representing data as a linear combination of products of corresponding functions of time and space.

There are many orthogonal functions that could be generated from any data set, but empirical eigenfunctions are most appropriate for this type of study. Other orthogonal expansions (e.g., Fourier series) impose a functional form (such as a sinusoid — chosen a priori) on the data. Eigenfunction analysis provides the most efficient method of representing the data, since the first n terms in the series explain more of the data variability than the first n terms in any other expansion. Removing the lower-ranked eigenfunctions,

which are presently physically uninterpretable, statistically insignificant, and have negligible impact on the beach profile, in a sense removes the "noise" (less predictable part of the data) from the data set (see Overland and Preisendorfer, 1982).

We represent the height of the profile as:

$$h_{xt} = \bar{h}_x + \sum_{n=1}^{N} a_n c_{nt} e_{nx} \tag{1}$$

where h_{xt} is the height of the profile at point x and time t, $\bar{h}_x$ is the mean profile height at point x, c_{nt} are the temporal eigenfunctions, and e_{nx} are the spatial eigenfunctions. N is the number of eigenfunctions in the series.

The e_n are eigenfunctions (eigenvectors) computed from the spatial covariance matrix **A**:

$$\mathbf{A} = \frac{1}{n_x n_t} (\mathbf{H}\mathbf{H}^T) \quad (n_x, n_x) \tag{2}$$

where superscript T is the transpose operator, n_x equals the number of spatial points per profile, n_t is the number of profiles, and **H** is formed of the profile data elements h_{xt} minus the profile mean $\bar{h}_x$.

Rather than covariance matrices, Winant et al. (1975) and Aubrey (1979) use sum of square and cross products matrices (SSCP) in which the mean has not been removed from the data. Because of this, their 1st eigenfunction is analogous to the mean beach profile $\bar{h}_x$ of this study, and their 2nd, 3rd and 4th eigenfunctions are analogous to the 1st, 2nd and 3rd eigenfunctions, respectively, used here.

The c_n are the eigenfunctions computed from the temporal covariance matrix **B**, where:

$$\mathbf{B} = \frac{1}{n_x n_t} (\mathbf{H}^T\mathbf{H}) \quad (n_t, n_t) \tag{3}$$

The eigenvalues (λ_n) and eigenvectors are defined by the equations:

$$\mathbf{A}_n\mathbf{e}_n = \lambda_n\mathbf{e}_n \tag{4}$$

$$\mathbf{B}_n\mathbf{c}_n = \lambda_n\mathbf{c}_n \tag{5}$$

The scaling factors, which have units of length, are defined as:

$$a_n = (\lambda_n n_x n_t)^{1/2} \tag{6}$$

Although **A** and **B** may be of different rank, they will have the same non-trivial eigenvalues. Hence, they will have the same number of non-zero eigenfunctions, N, equal to the lesser of n_x and n_t.

The first two temporal eigenfunctions are plotted against each other in Cartesian coordinates ($c_i c_j$ plots) to examine their dominant cycles of beach change. To remove effects of long-term accumulation or loss of sand on the beaches studied, a linear trend was removed from each temporal eigenfunction before further analysis.

Rotary component analysis (Gonella, 1972) is applied to the (c_i, c_j) vector pair to delineate the spectral energy density and associated beach cycles. Examples of rotary component analysis as applied to physical oceanographic data are presented in Gonella (1972) and Mooers (1970). These references may be useful to those unfamiliar with this analytical method. A beach cycle will be defined for each frequency with a statistically significant peak. Each significant frequency will have a rotary sense defined in the (c_i, c_j) vector space; this rotary motion will define the sequence of cyclical beach change in eigenspace. Beach profiles corresponding to these rotary motions (cycles) can then be reconstructed using eqn. (1). The result is a quantitative, statistical description of cycles in beach state. To make the data suitable for rotary component analysis, the temporal eigenfunctions are interpolated so the number of profiles represented is an integral power of 2, and so the profiles are uniformly spaced in time (Table 1). An alternative interpolation could take place with the original data, before calculating principal components. The former technique is preferred to avoid altering the original measured data matrix.

Each frequency for each $c_i c_j$ plot has a rotary (elliptical) motion indicating the dominant cyclical direction of beach change. Given the area of the ellipse, its eccentricity, its orientation with respect to the axes, and its center (the mean value of the eigenfunctions), one can define the ellipse and its position in (c_i, c_j) vector space. These quantities can be derived through partitioning of the mean energy into energy associated with clockwise and counterclockwise motion on the ellipse. The dominant of the two energies governs the sign of the angular frequency, the direction of motion in eigenspace.

For a two-dimensional vector field, one defines a complex vector:

$$c = c_i + i\, c_j$$

where:

$$i = \sqrt{-1}$$

TABLE 1

Five profile sequences for Torrey Pines Beach, California

Profile	Original no. of profiles	No. after interpolation	Interval of measurements	Time interval between interpolated profiles
Indian Canyon Range	62	64	6/72—11/77	30.44 days
South Range	62	64	6/72—11/77	30.44 days
Indian Canyon Range	39	32	12/75—1/77	13.31 days
South Range	55	64	12/75—1/77	6.68 days
North Range	55	64	12/75—1/77	6.68 days

These can be transformed in a Fourier sense:

$$c_\omega = \frac{1}{T} \int_0^T c(t)\, e^{-i\omega t} dt = |c_\omega|\, e^{i\theta\omega}$$

where T is the record duration. c_ω yields the amplitude $|c_\omega|$ and phase θ_ω for both positive (anticlockwise) and negative (clockwise) frequencies. The total spectrum is:

$$S_t = S_- + S_+ = \tfrac{1}{4} \{P_{c_i} + P_{c_j}\}$$

where S_- is the clockwise spectrum, S_+ is the anticlockwise spectrum, P is the cospectrum, and Q is the quadrature spectrum.

$$S_- = \langle c_-^* \, c_- \rangle / 2 = \frac{1}{8} \{P_{c_i} + P_{c_j} - 2Q_{c_i c_j}\}$$

$$S_+ = \langle c_+^* \, c_+ \rangle / 2 = \frac{1}{8} \{P_{c_i} + P_{c_j} + 2Q_{c_i c_j}\}$$

where the brackets ($\langle\ \rangle$) represent ensemble (or piece-wise) averages. The rotary coefficient:

$$R = (S_- - S_+)/(S_t) = \frac{(-2Q_{c_i c_j})}{(P_{c_i} + P_{c_j})}$$

defines the rotary extent; it is one for pure rotary motion and zero for unidirectional motion. It is related to the ellipticity, ϵ, by:

$$R = 1 - \epsilon$$

the orientation of the major axis of the ellipse is:

$$\theta = \frac{\theta_+ + \theta_-}{2} + k\pi = \tan^{-1} \left[\frac{(2P_{c_i c_j})}{(P_{c_i} - P_{c_j})} \right]$$

The stability of the ellipse can also be defined, with confidence limits identical to that for coherence (Gonella, 1972).

The total spectrum, S_t, determines the significant frequencies in each $c_i c_j$ plot. Because we calculate the spectrum of a normalized eigenvector, the total energies of the two eigenvectors will be the same; however, a relative peak in the mean energy caused by a lower-ranked eigenfunction will be relatively less important to the morphology of the beach profile than a similar size peak caused by a higher-ranked eigenfunction. This is because of the lower magnitude of the eigenvalue associated with the lower ranked eigenfunction, which is a factor in the formula for profile reconstruction [eqn. (1)]. Because the temporal eigenfunctions have been demeaned and interpolated, they are no longer exactly normalized nor orthogonal to each other. Points chosen from the ellipse (the endpoints of the major and minor axes and the endpoints of the latera recta) define reconstructed profiles [eqn. (1)], representing the beach cycle for a particular frequency.

RESULTS AND DISCUSSION

The first three spatial eigenfunctions have similar shapes for all five data sets (Figs.2 and 3). The first spatial eigenfunction shows a maximum near the shore and minimum offshore. The second spatial function has a broad maximum over the zero-crossing of the first eigenfunction. The third has maxima and minima in the same areas of maxima and minima of the first two eigenfunctions.

The first temporal eigenfunction shows a periodicity of about 1 year, representing seasonal onshore/offshore movement of sediment. The time dependence of the second eigenfunction is more complicated, consisting of a weak seasonality with superimposed higher-frequency changes. The second temporal eigenfunction describes how the beach oscillates between a berm and a bar profile, because the first eigenfunction, a standing wave, cannot describe the progressive motion of the sand (Aubrey, 1979). Spectral eigenanalysis (e.g., Brillinger, 1981) would improve the description of onshore—offshore sediment exchange.

Because the first and second eigenfunctions account for a large percentage (between 65 and 90%) of the variability of the data (Table 2), the beach profiles are approximated by these two variables and the mean profile. As a result, rotary component analysis is applied only for the pairing of the first and second temporal eigenfunctions. Tests of statistical confidence levels

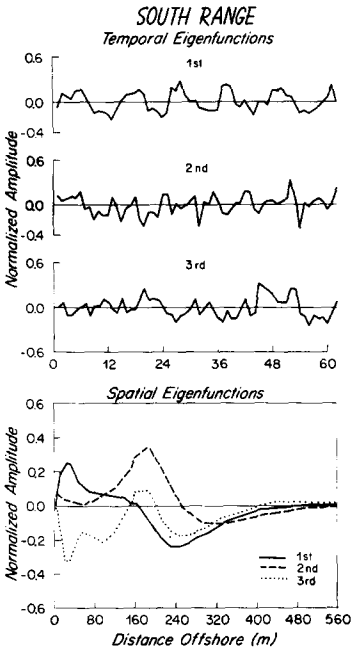

Fig.2. Spatial and temporal eigenfunctions for South Range over the period June 1972—November 1977. Units for temporal eigenfunctions are elapsed time, in months.

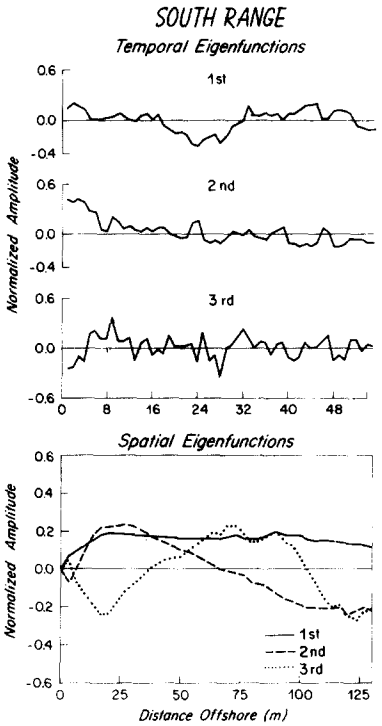

Fig.3. The spatial and temporal eigenfunctions for South Range over the period December 1975—January 1977. Units of temporal eigenfunctions are elapsed time, in weeks.

TABLE 2

Percentage of the mean square deviation explained by the first three eigenfunctions

	Eigenfunction No.	Indian Canyon	South Range	North Range
One-year	1	76.4	70.7	74.6
data sets	2	14.6	14.6	12.7
	3	4.4	5.2	4.2
Total MSV		95.4	90.5	91.5
Five-year	1	42.1	46.2	
data sets	2	24.3	19.6	
	3	11.4	12.4	
Total MSV		77.8	78.2	

(Preisendorfer et al., 1981) indicate that the first and second eigenvectors are significantly different from noise.

The first and second temporal eigenfunctions (with a linear temporal trend removed) were plotted against each other, component versus component, to examine patterns in their change. Clusters of points should indicate a profile

near equilibrium (a favorable beach state), while long line segments connecting the clusters would signify less frequent, large changes in a profile, perhaps due to a sudden change in wave activity. The month corresponding to each data point is plotted to determine if there are characteristic eigenfunction pairs associated with certain periods of the year (Figs.4 and 5).

Points representing profiles from the months of August through December (8—12) are consistently found in quadrants I and IV (positive c_1). These months are generally associated with the buildup then erosion of a berm

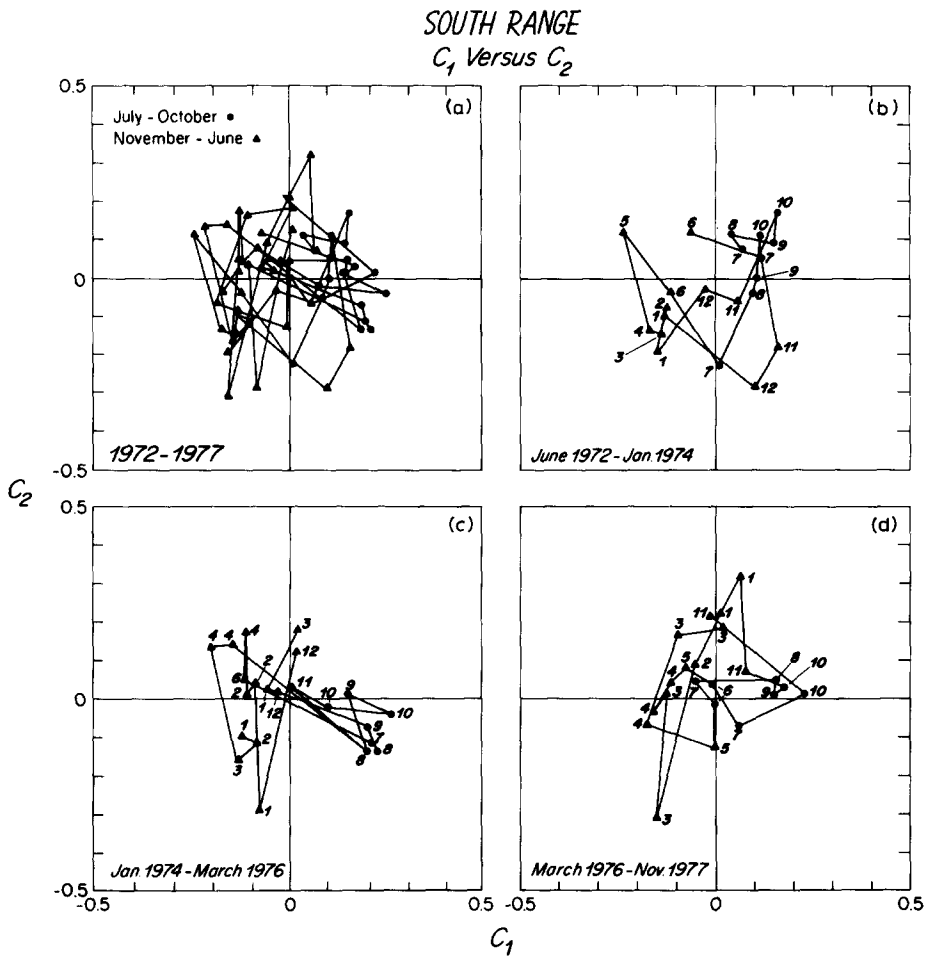

Fig.4.(a) Temporal eigenfunction 1 plotted against temporal eigenfunction 2 for South Range for the period June 1972—November 1977. (b) Temporal eigenfunction 1 plotted against temporal eigenfunction 2 for South Range for the period June 6, 1972—January 22, 1974 (using data for June 1972—November 1977). (c) Temporal eigenfunction 1 plotted against temporal eigenfunction 2 for South Range for the period January 22, 1974—March 4, 1976. (d) Temporal eigenfunction 1 plotted against temporal eigenfunction 2 for South Range for the period March 4, 1976—November 9, 1977.

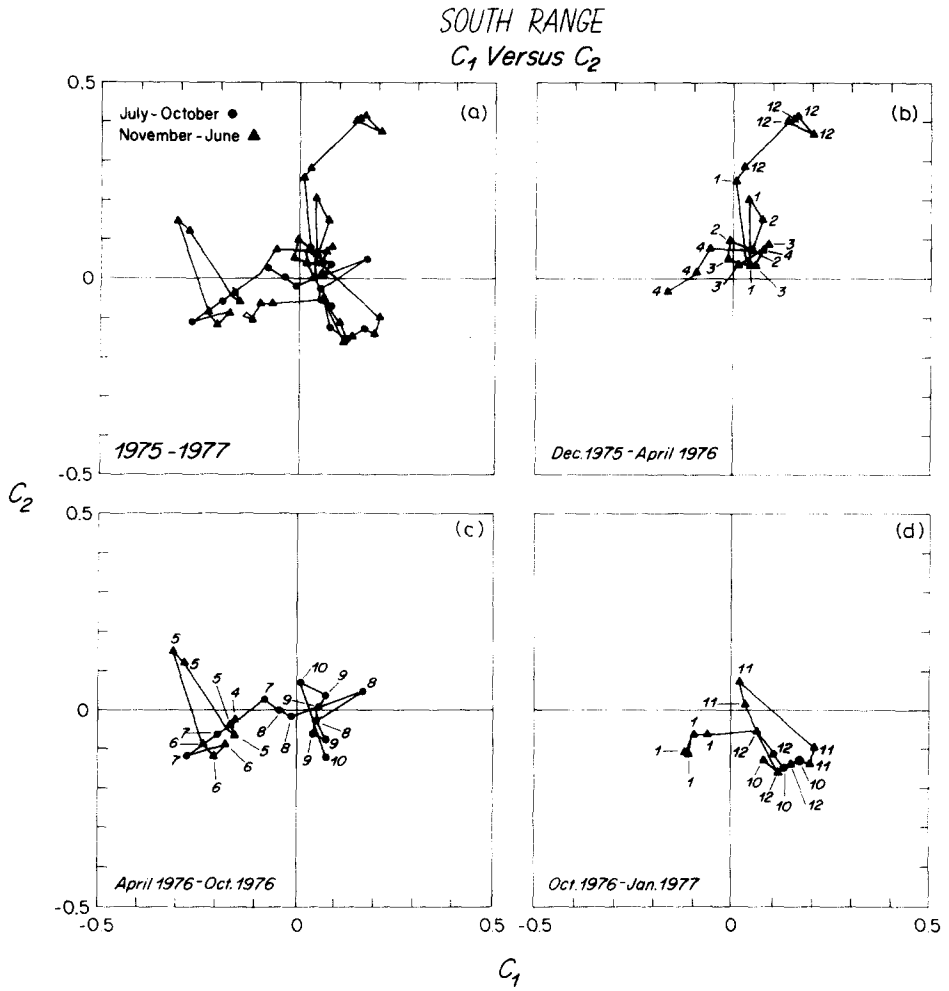

Fig.5.(a) Temporal eigenfunction 1 plotted against temporal eigenfunction 2 for South Range for the period December 1975—January 1977. (b) Temporal eigenfunction 1 plotted against temporal eigenfunction 2 for South Range for the period December 1, 1975—April 28, 1976 (using data set for December 1975—January 1977). (c) Temporal eigenfunction 1 plotted against temporal eigenfunction 2 for South Range for the period April 28, 1976—October 7, 1976. (d) Temporal eigenfunction 1 plotted against temporal eigenfunction 2 for South Range for the period October 7, 1976—January 26, 1977.

profile in southern California (Aubrey et al., 1980). The months February through June (2—6) are generally located in quadrants II and III (negative c_1), and are the months often associated with disappearance then formation of a berm profile. January and July are times of transition in the profile from berm-to-bar and bar-to-berm.

Rotary motion is observable on plots of c_1 vs. c_2. This motion, complex in frequency, can be separated into many elliptical components, each representing

a particular frequency associated with the temporal eigenfunctions. Rotary component analysis shows a frequency of about one cpy contained approximately an order of magnitude more energy than any other frequency (between 50 and 60% of the total energy; Fig.6). Most of this energy is attributable to the one-year periodicity of the first eigenfunction. A half-year cycle is also significant in the five year data set, but has less relative energy (between 6 and 20% of the total energy). Mean elliptical paths are defined by rotary components for both annual and semi-annual frequencies. Sequential sets of profiles are constructed for each frequency by substituting points from the perimeter of the ellipses into eqn. (1), for $N = 2$.

Results from the two five-year data sets clearly demonstrate the one-year cycle of sediment transport from offshore bar to onshore berm (Figs.7 and 8). Each beach profile sequence is associated with an ellipse of large eccentricity (ellipticity of about 0.6, average) and slightly positive slope of the major axis (Fig.7). Because of this, the cycle is dominantly affected by c_1 values, which oscillate between positive and negative; the role of c_2, which should theoretically control the oscillation between bar and berm profiles, has a fairly limited range of near-zero values and plays a smaller role in determining the beach profile shape. In agreement with the original c_1c_2 plots, the "berm" profiles are associated with positive c_1 (and generally positive c_2; quadrant I). The "bar" profile is associated with negative c_1 (and negative c_2; quadrant III).

As an example, the sequence from South Range (Fig.8a, approximately an October profile) shows a well-developed berm and shallow offshore trough. Gradually, as sediment moves offshore due to winter wave conditions, the berm disappears and the trough gets smaller (Fig.8b, approximately January). As the sediment continues to move offshore, the area of the former berm becomes a shallow beach face and a small bar develops offshore. The beach face takes on its smallest slope in Fig.8c (approximately April). Afterwards, sediment begins moving onshore, a small berm reappears, and the bar moves shoreward (Fig.8d, approximately July).

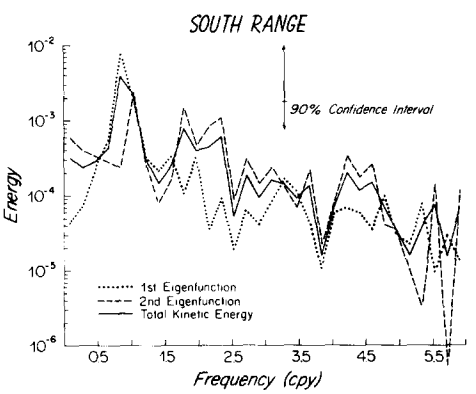

Fig.6. Spectral analysis of first and second temporal eigenfunctions for South Range for the period of June 1972—November 1977.

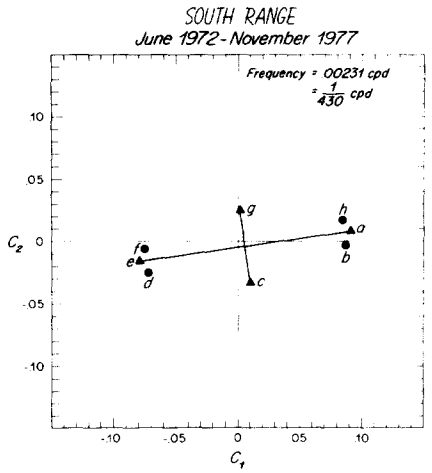

Fig.7. End points of major and minor axes and latera recta of mean elliptical path in eigenspace — annual beach cycle for South Range for the period June 1972 — November 1977.

Finally the berm enlarges, the bar moves all the way onshore and a trough begins to take its place offshore (approximately September). Changes in the onshore profile appear to lag by a small time change in the offshore profile.

The ellipse associated with the semi-annual cycle from both Indian Canyon and South Range is relatively smaller and has a wider range of c_2 values relative to c_1 values than the ellipse connected with the annual cycle (ellipticity averages 0.12; Figs.9 and 10). The effect of the semi-annual cycle on the reconstructed profiles is accordingly greatest over the first pivotal point of Aubrey (1979), where c_2 is at its maximum. This clearly shows its role in controlling the fluctuations between bar and berm profile.

The one-year data sets also have peak energies around one cpy, although poorly resolved. The ellipses associated with this frequency had little ellipticity and a slightly negative slope to the c_1 axis for all three data sets. Using South Range as an example, we see in July a small trough located about 45 m offshore, and a region with values greater than the mean profile past about 55 m offshore. In succeeding profiles, sand moves onshore to fill the trough and form a small berm (approximately October), it enlarges the berm and decreases the profile heights from 100 m onward, and finally it forms an area beyond 75 m with profile elevations less than the mean profile. Sediment begins moving seaward with the coming of winter weather, decreasing the size of the berm and continuing to lessen the profile height past about 55 m (around January). Finally, the berm disappears and the entire profile becomes lower than the mean profile (approximately April). Sediment continues to move offshore until the original berm area is a small trough; the sand removed from that trough, transported seaward, causes profile elevations past about 75 m to be higher than the mean profile elevations.

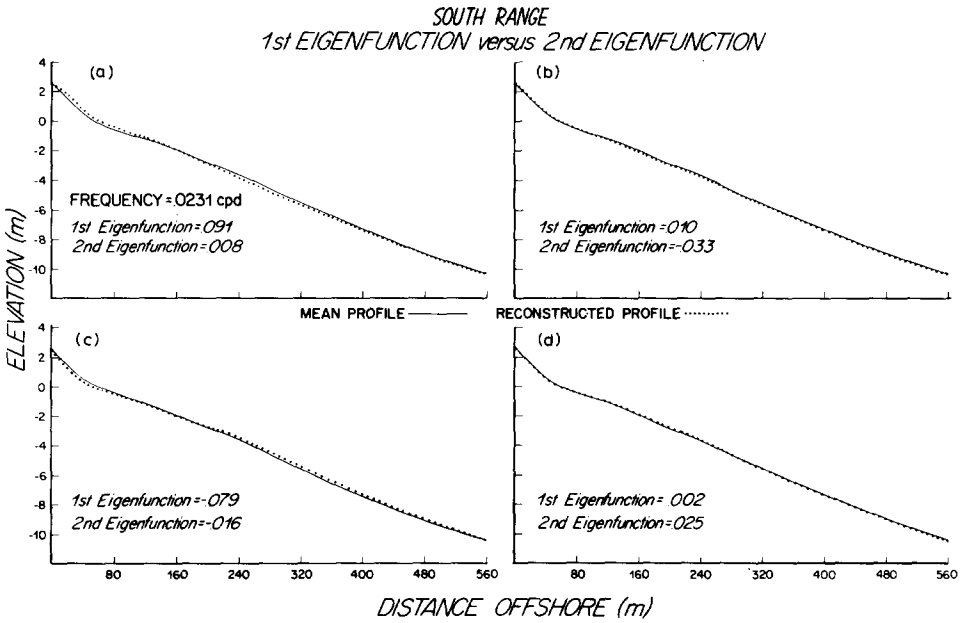

Fig.8. Annual beach cycle for South Range for the period June 1972—November 1977. Profiles are reconstructed at the points in Fig.7.

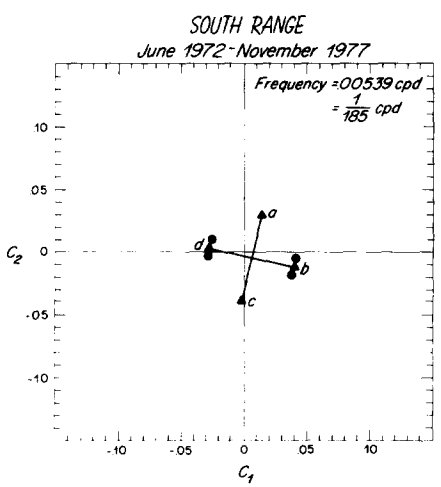

Fig.9. End points of major and minor axes and latera recta of mean elliptical path in eigenspace — semi-annual beach cycle for South Range for the period June 1972 — November 1977.

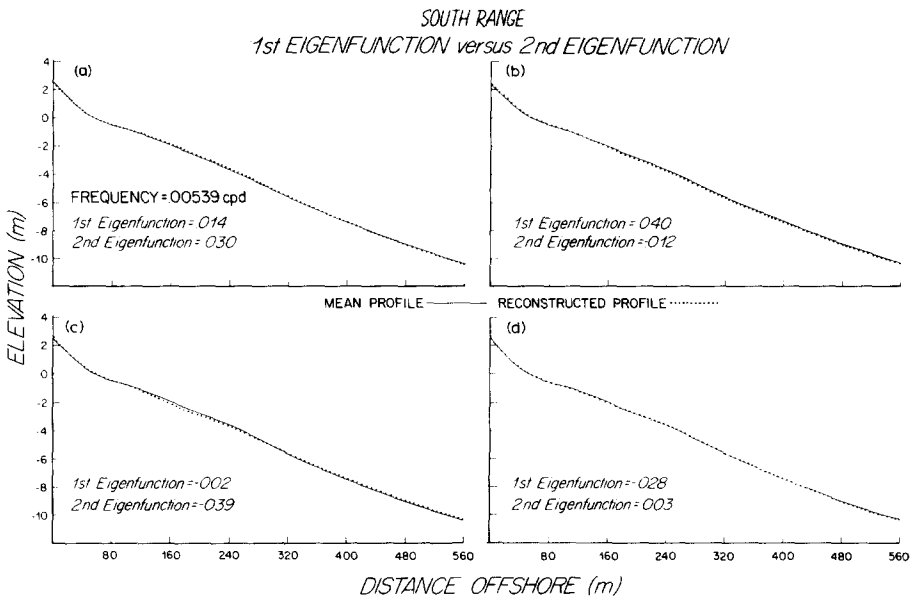

Fig.10. Semi-annual beach cycle for South Range for the period June 1972—November 1977. Profiles are reconstructed at the endpoints of the major and minor axes in Fig.9.

The one-year data sets do not have a strong semi-annual beach cycle. Spectral analysis also shows relatively little energy associated with a monthly (lunar) cycle.

CONCLUSIONS

The large percentage of data variability explained by the first and second eigenfunctions allows the beach profiles to be accurately reconstructed with only these two functions and the mean profile. Plots of the first versus the second temporal eigenfunction exhibit complex cyclicity corresponding to the sequential change of beach profiles through time. It is possible to represent this cyclicity by assigning a mean rotary motion to each frequency. The most energetic frequencies are associated with the largest ellipses and have the greatest effect on the cycle of beach profile changes. From the ellipses one can reconstruct a series of profiles corresponding to the onshore/offshore sediment movement associated with the particular frequency. Ideally, one might like to construct a sequence of beach profile changes analogous to those described qualitatively by Sonu and Van Beek (1971), Short (1979), and Wright et al. (1979).

Spectral analysis demonstrates a frequency of one cycle per year to be the most dominant for all data sets (both five-year and one-year). The sequence of reconstructed profiles for this frequency mimics the seasonal onshore/offshore migration of sand. Because of the dominance of this frequency, the corresponding profile sequence fairly accurately represents a typical beach cycle.

A frequency of two cpy in the five-year data sets has the only other statistically significant energy peak in the spectral analysis. The semi-annual beach cycle has its greatest effect on the area of the beach near the first pivotal point of Aubrey (1979). Although ordinarily its effect might be partially masked by the annual cycle, the semi-annual cycle clearly plays a role in the oscillations between bar and berm profile.

The processes responsible for these cyclical beach changes are discussed in detail in Aubrey (1978) and Aubrey et al. (1980). Beach changes reflect the strong annual periodicity in the wave climate, with a low-amplitude, long-period (hence low steepness) wave climate during the late spring, summer, and early fall, and a large-amplitude (higher steepness) wave climate dominating the remainder of the time. Statistical relationships between beach response to incident wave action is well documented; continued work is required to improve our understanding of the dynamics of these processes.

The methods used in this study are a concise way to model and predict beach cycles. With little modification they can be applied to three-dimensional beaches. A separate empirical eigenfunction analysis and rotary component analysis will be necessary to quantify profile cycles on any particular beach. However, general models of on-offshore sediment transport can be verified through analysis of data from a varied selection of beaches; the method provides a uniform standard for intercomparing these beach changes. A more exhaustive study with a greater variety of beach profile data should greatly increase the understanding of beach cycles.

Improvements to this methodology include use of spectral eigenfunction analysis, to properly describe the propagating wave-like sediment exchange between the bar and berm.

ACKNOWLEDGEMENTS

This work was supported in part by the Office of Sea Grant, Grant number NA80-AA-D-00077, as part of the Nearshore Sediment Transport Study; by the Woods Hole Oceanographic Institution's Coastal Research Center; and by the W.H.O.I. Education Office (which supported R.M.R. as a Summer Student Fellow in 1983). G.P. Lohmann and D. Lazarus commented on earlier versions of this manuscript.

REFERENCES

Aubrey, D.G., 1978. Statistical and dynamical prediction of changes in natural sand beaches. Ph.D. thesis, Scripps Inst. of Oceanogr., San Diego, Calif., 194 pp.

Aubrey, D.G., 1979. Seasonal patterns of onshore/offshore sediment movement. J. Geophys. Res., 84: 6347—6354.

Aubrey, D.G., Inman, D.L. and Winant, C.D., 1980. The statistical prediction of beach changes in southern California. J. Geophys. Res., 85: 3264—3276.

Brillinger, D.R., 1981. Time Series: Data Analysis and Theory. Holden-Day, San Francisco, Calif., 540 pp.

Gonella, J., 1972. A rotary-component method for analyzing meteorological and oceanographic vector time series. Deep-Sea Res., 19: 833—846.

Mooers, C.N.K., 1970. The interaction of an internal tide with the frontal zone of a coastal upwelling region. Ph.D. thesis, Oregon State Univ., Corvallis, Oreg.

Nordstrom, C.E. and Inman, D.L., 1975. Sand level changes on Torrey Pines Beach, California. Beach Erosion Board, U.S. Army Corps Eng., Misc. Pap. 11—75, 166 pp.

Overland, J.E. and Preisendorfer, R.W., 1982. A significance test for principal component applied to a cyclone climatology. Mon. Weather Rev., 110: 1—4.

Preisendorfer, R.W., Zwiers, F.W. and Barnett, T.P., 1981. Foundations of principal components selection rules. SIO Ref. Ser. No. 81—4, 192 pp.

Ross, R.M., 1983. A quantitative description of beach cycles at Torrey Pines Beach, Southern California. Woods Hole Oceanogr. Inst., unpubl. manuscr., 118 pp.

Shepard, F.P., 1950. Beach cycles in southern California. Beach Erosion Board, U.S. Army Corps Eng., Tech. Memo. 20, 26 pp.

Short, A.D., 1979. Three dimensional beach-stage model. J. Geol., 87: 553—571.

Sonu, C.J. and Van Beek, J.L., 1971. Systematic beach changes on the Outer Banks, North Carolina. J. Geol., 79: 416—425.

Wayland, R.J., 1983. Shorezone profile dynamics. M.Sc. thesis, Univ. of Virginia, Charlottesville, Va., 66 pp.

Winant, C.D., Inman, D.L. and Nordstrom, C.E., 1975. Description of seasonal beach changes using empirical eigenfunctions. J. Geophys. Res., 80: 1979—1986.

Wright, L.D., Chappell, J., Thom, B.G., Bradshaw, M.P. and Crowell, P., 1979. Morphodynamics of reflective and dissipative beach and inshore systems, southeastern Australia. Mar. Geol., 32: 105—140.

Wright, L.D., Short, A.D. and Nielsen, P., 1982. Morphodynamics of high energy beaches and surf zones: A brief synthesis. Coastal Studies Unit Tech. Rept. No. 82/5, Coastal Studies Unit, Univ. of Sydney, Sydney, N.S.W., 64 pp.